



# Long-Term Evolution of Neptune Trojans

E. Tello Huanca<sup>1</sup>, R.P. Di Sisto<sup>1,2</sup> y A. Brunini<sup>1,2</sup>

<sup>1</sup>Facultad de Ciencias Astronómicas y Geofísicas, UNLP, Paseo del Bosque S/N (1900), La Plata, Argentina

<sup>2</sup>IALP- CCT La Plata-CONICET-UNLP Paseo del Bosque S/N (1900), La Plata, Argentina.

CONICET



## Resumen

Los Trojanos de Neptuno son objetos que comparten la órbita con el planeta Neptuno y se encuentran en un entorno de los puntos de Lagrange L<sub>4</sub> y L<sub>5</sub> situados 60° “delante” y 60° “detrás” del planeta en su órbita. Hasta el momento se han observado sólo nueve Trojanos de Neptuno. Sin embargo los estudios sobre la estabilidad de esta población indican que debería ser muy numerosa. En el presente trabajo realizamos simulaciones numéricas de la evolución de Trojanos de Neptuno ficticios, para detectar las zonas de estabilidad e inestabilidad de la población y estudiar cómo se produce el escape de los Trojanos a lo largo de la vida del Sistema Solar.

## Abstract

Neptune Trojans are objects that share the orbit with the planet Neptune and are in a neighborhood of the Lagrangian points L<sub>4</sub> and L<sub>5</sub> located 60° “front” and 60° “behind” the planet in its orbit. So far, there have been discovered only nine Neptune Trojans. However stability studies indicate that this population should be large. In this work we report the results of numerical simulations of the evolution of fictitious Neptune Trojans, to detect areas of stability and instability and also to study the escape of Trojans over the age of the Solar System.

## INTRODUCTION

The first Neptune Trojan was discovered in 2001 around L<sub>4</sub> and was named 2001 QR322. Since then it has been discovered 5 more in L<sub>4</sub> and only 3 in L<sub>5</sub>. Table 1 shows the Neptune Trojans discovered to date.

Prov.	Des.	Ln	q	Q	H	Epoch	M	Peri.	Node	Incl.	e	a
2004	UP10	L4	29.32	31.1	8.8	20131104	345	6	34.8	1.4	0.029	30.209
2005	TO74	L4	28.54	31.9	8.5	20131104	279	302.7	169.4	5.3	0.055	30.197
2001	QR322	L4	29.46	31.1	8.2	20131104	66.34	163.4	151.6	1.3	0.027	30.285
2004	KV18	L5	24.54	35.7	8.9	20131104	63.33	294.4	235.6	13.6	0.186	30.138
2005	TN53	L4	28.13	32.3	9	20131104	297.4	86.5	9.3	25	0.068	30.2
2006	RJ103	L4	29.18	31.1	7.5	20131104	256.3	20.6	121	8.2	0.031	30.121
2007	VL305	L4	28.13	32.2	8	20131104	0.91	218.3	188.6	28.1	0.067	30.15
2008	LC18	L5	27.31	32.5	8.4	20131104	174.6	8.6	88.5	27.6	0.086	29.894
2011	HM102	L5	27.68	32.4	8.1	20131104	25.69	151.1	101	29.4	0.079	30.035

Table 1: Neptune Trojans discovered to date (Sept. 2014) (<http://www.minorplanetcenter.net>)

There are several works concerning the formation, origin and stability of Neptune Trojans and in generally they suggest that they should be a relatively large population, even bigger than Jupiter Trojans. Sheppard & Trujillo (2010) performed a “survey” with the 8.2 Subaru telescope and the 6.5 m Magellan telescope, detecting 5 Trojans in L<sub>4</sub> and 1 in L<sub>5</sub>. From this work, the authors derived the cumulative size distribution (CSD) of Neptune Trojans. Assuming an albedo of 0.05, Sheppard & Trujillo (2010) estimated that the CSD is given by  $N(>D) \propto D^{-4}$  for objects with diameters  $D > 45$  km and in  $D \sim 45$  km, it has a break, analogous to that found in other populations of small bodies. They also estimate that there could be about 400 Neptune Trojans with diameters  $D > 100$  km.

Neptune Trojans are a stable population, and therefore a large number of objects is expected to survived for the age of the Solar System. In this work we study the stability of this population to detect Trojans that can escape and would be part of other populations of small bodies in the Solar System.

## NUMERICAL SIMULATION

The first work stage involves the numerical integration of fictitious Trojans in the resonance. To do this we take as a reference the works of Zhou et al. (2009, 2010). In the first paper, the authors studied the orbits of Neptune Trojans, providing a view of the stability of the population according to inclination. They also show stability maps where one can observe three stable regions with inclinations between the intervals: (0°, 12°), (22°, 36°) and (51°, 59°), where it would be expected to find Trojans. In the second paper, the authors study the global stability of Neptune Trojans depending on the eccentricity and inclination. To do this, Zhou et al. (2010) perform numerical simulations in order to obtain the dependence the libration center ( $\sigma_c$ ) with the eccentricity and inclination. In Figure 1 we show their results.

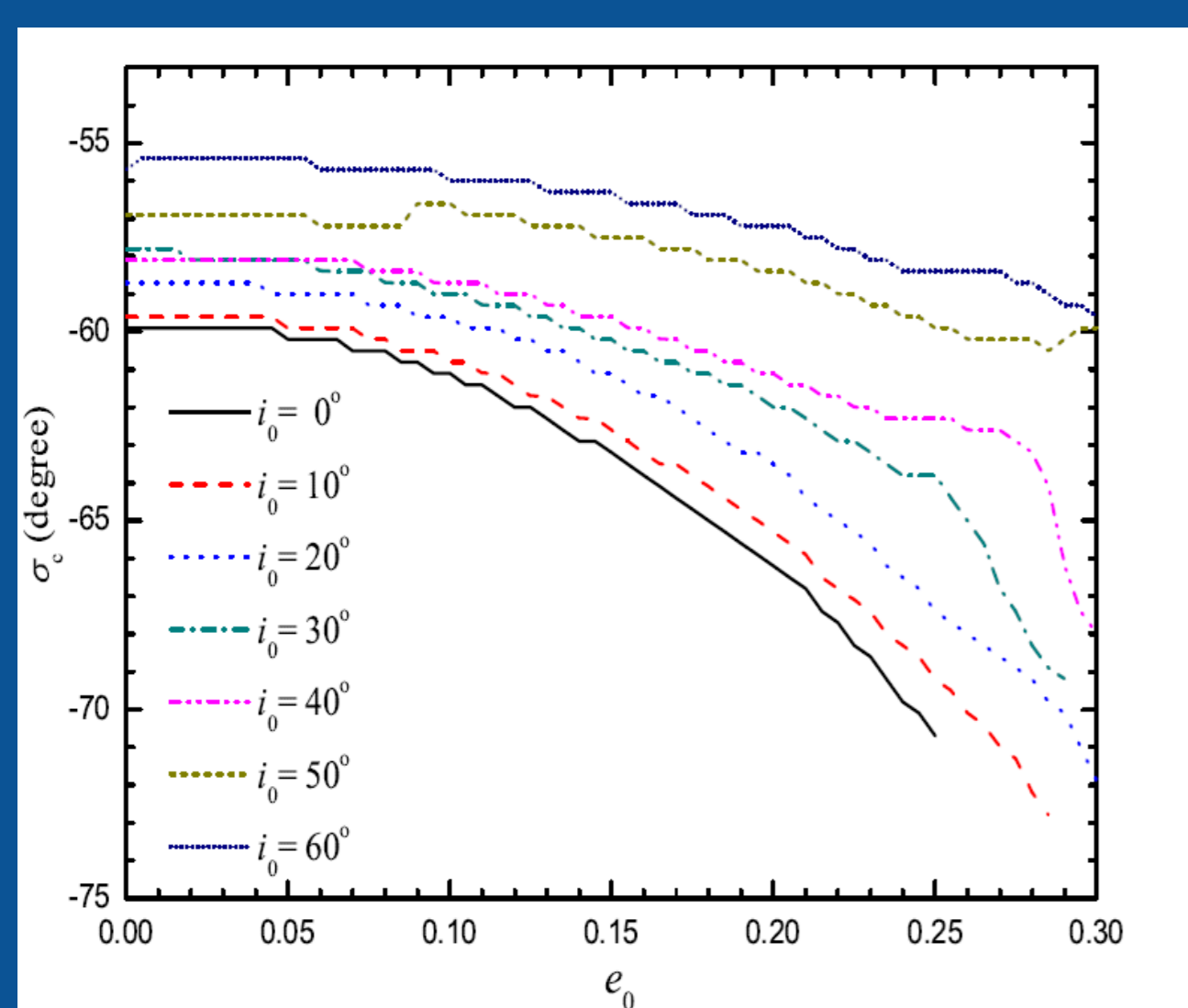


Figure 1: Variation of libration center ( $\sigma_c$ ) with respect to the eccentricity and inclination (from Zhou et al., 2010).

The initial orbital elements of fictitious Trojans were taken Zhou et al. (2009, 2010) taking into account the values of  $\sigma_c$  from Figure 1. For Trojans around the Lagrange point L<sub>5</sub> we define a grid of orbital elements of widths  $\Delta e = 0.01$  ( $e$  = eccentricity),  $\Delta a = 0.01$  AU ( $a$  = semimajor axis) and  $\Delta i = 2.5^\circ$  ( $i$  = inclination), with  $29.9$  AU  $\leq a \leq 30.49$  AU,  $0 \leq e \leq 0.25$  and  $0^\circ \leq i \leq 60^\circ$ . The argument of perihelion  $\omega = \omega_N - 60^\circ$ , the longitude of ascending node  $\Omega = \Omega_N$  and the mean anomaly  $M = M_N + 60^\circ + \sigma_c$ , where  $\sigma_c$  is obtained from Figure 1. and the subscript N corresponds to Neptune. Similarly we obtained the orbital elements for the Trojans around the Lagrangian point L<sub>4</sub>.

In total, we have 31380 orbits of fictitious Trojans around each Lagrange point (L<sub>4</sub> and L<sub>5</sub>), that come into our numerical simulation.

We use the numerical code EVORB (Fernández et al 2002.), to integrate our fictitious Trojans (massless particles) under the gravitational action of the Sun and the four giant planets: Jupiter, Saturn, Uranus and Neptune, with a step of 0.5 years and for  $4.5 \times 10^9$  years. To manage such a big number of particles we use several processors that run for a period of approximately 2-4 months. The cutoff criteria for the program, is an encounter with a planet at a distance less than 1 Hill radius, ejection or collision with a planet or the Sun.

## RESULTS

Of the 31380 initial particles in each Lagrange point, 83% and 82% escaped from the L<sub>4</sub> and L<sub>5</sub> Trojan population, respectively because of an encounter with a planet and the rest remained in the integration up to the end of the simulation. From the particles that escaped from L<sub>4</sub> and L<sub>5</sub> respectively, 69.25% and 71.5% did by having encounters with Neptune, 30.74% and 28.48% by encounters with Uranus, and a small fraction of 0.0038% and 0.0032% with Saturn. From the output files of our simulation, we calculate the number of escape particles with respect to the number of survivors and plotted this ratio as a function of time in Figure 2. We can see that at the beginning, there are a lot of particles that escape because the initial orbital elements cover a wider area and not only the stable real region of Trojans. Therefore this part of the curve is arbitrary. After 10<sup>9</sup> years the curve appears close to constant and then being significant. Fitting a linear relation  $Y(t) = st + b$  to this curve we can then estimate the current escape rate of the population. The slope values obtained after the fitting are given by:

$$s = 3.98746 \times 10^{-10} \pm 1.611 \times 10^{-12} \text{ year}^{-1} \text{ for L}_4, \text{ and} \\ s = 3.79652 \times 10^{-10} \pm 1.37 \times 10^{-12} \text{ year}^{-1} \text{ for L}_5$$

With intercept values of :

$$b = 3.20894 \pm 0.003965 \text{ for L}_4, \text{ and} \\ b = 3.05839 \pm 0.003392 \text{ for L}_5$$

The slope ( $s$ ) represent the current rate of escape of Neptune Trojans.

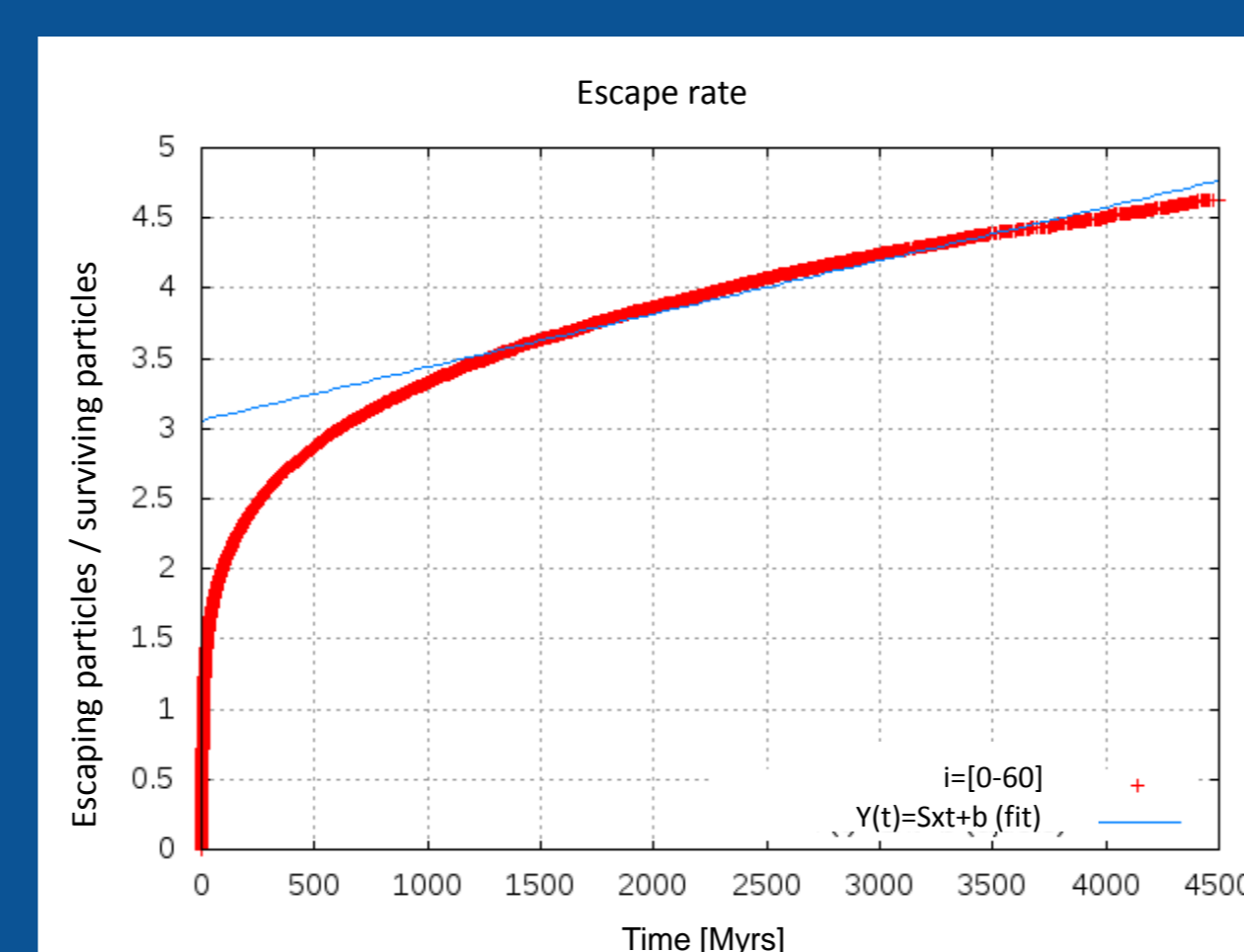
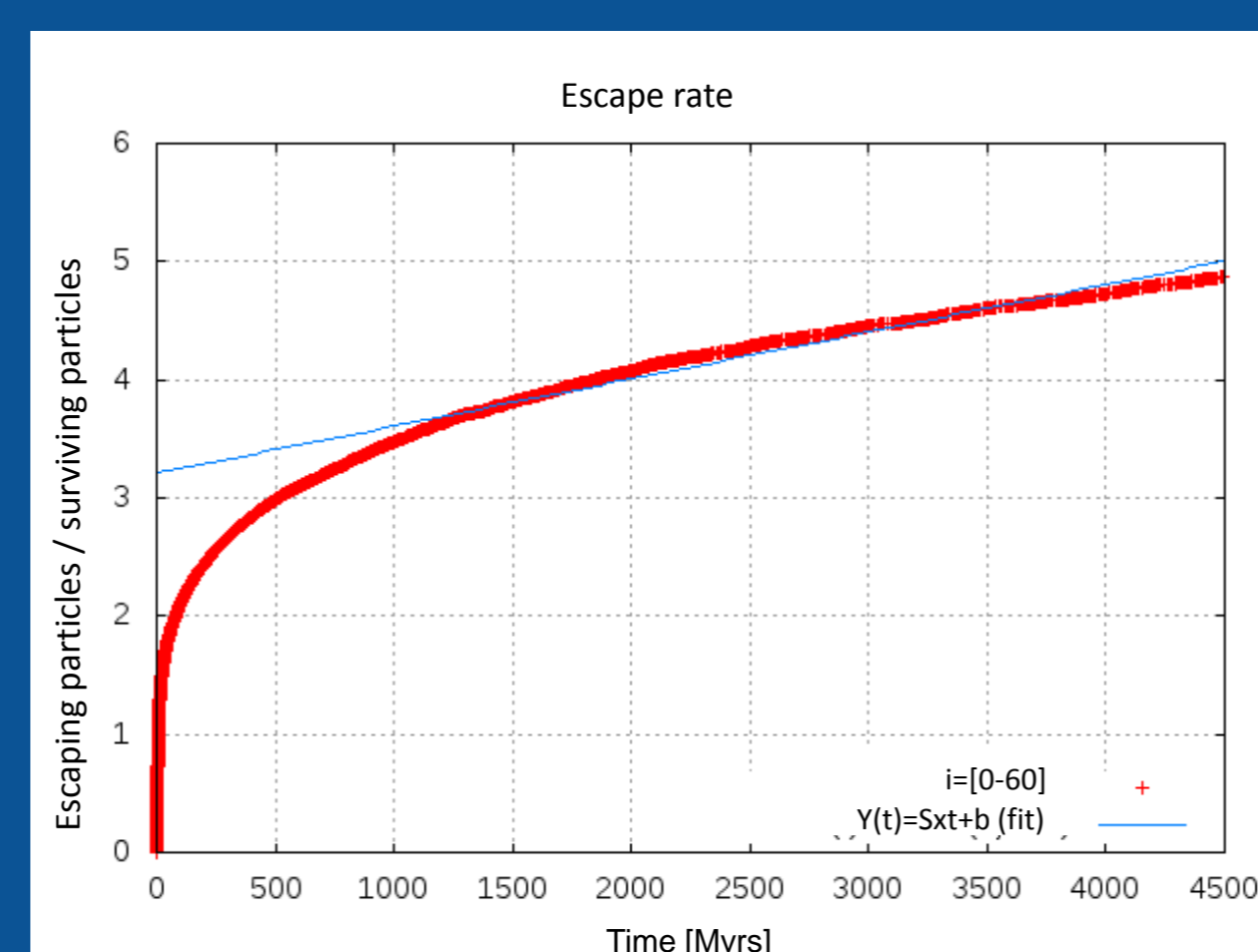


Figure 2: Top: Escape rate of particles around the Lagrangian point L<sub>4</sub>. Bottom: Escape rate of particles around the Lagrangian point L<sub>5</sub>.

Considering that there are 400 Trojans with diameters  $D > 100$  km (Sheppard & Trujillo 2010), then the rate of escape of Trojans with  $D > 100$  km is  $1.5 \times 10^7 \text{ yr}^{-1}$ , that is to say, that  $\sim 2$  Trojans greater than 100 km escape in 10<sup>7</sup> years, from each Lagrangian point. Taking as a reference the stability regions found by Zhou et al. (2009), we adopt these same regions to separate the particles in each one of them and group them according their initial inclination. In Figure 3 we plot the fraction of particles that escape from the different zones of stability defined by Zhou et al. (2009). We can observe that the most stable regions are between the range of inclination: (0°, 12°), (22°, 36°), (51°, 59°). After  $4.5 \times 10^9$  years, these three regions keep  $\sim 20\%$  of the initial objects. Moreover, the region of inclination (0°, 12°) result to be the most stable while the more unstable Trojans are those with  $i = 60^\circ$ .

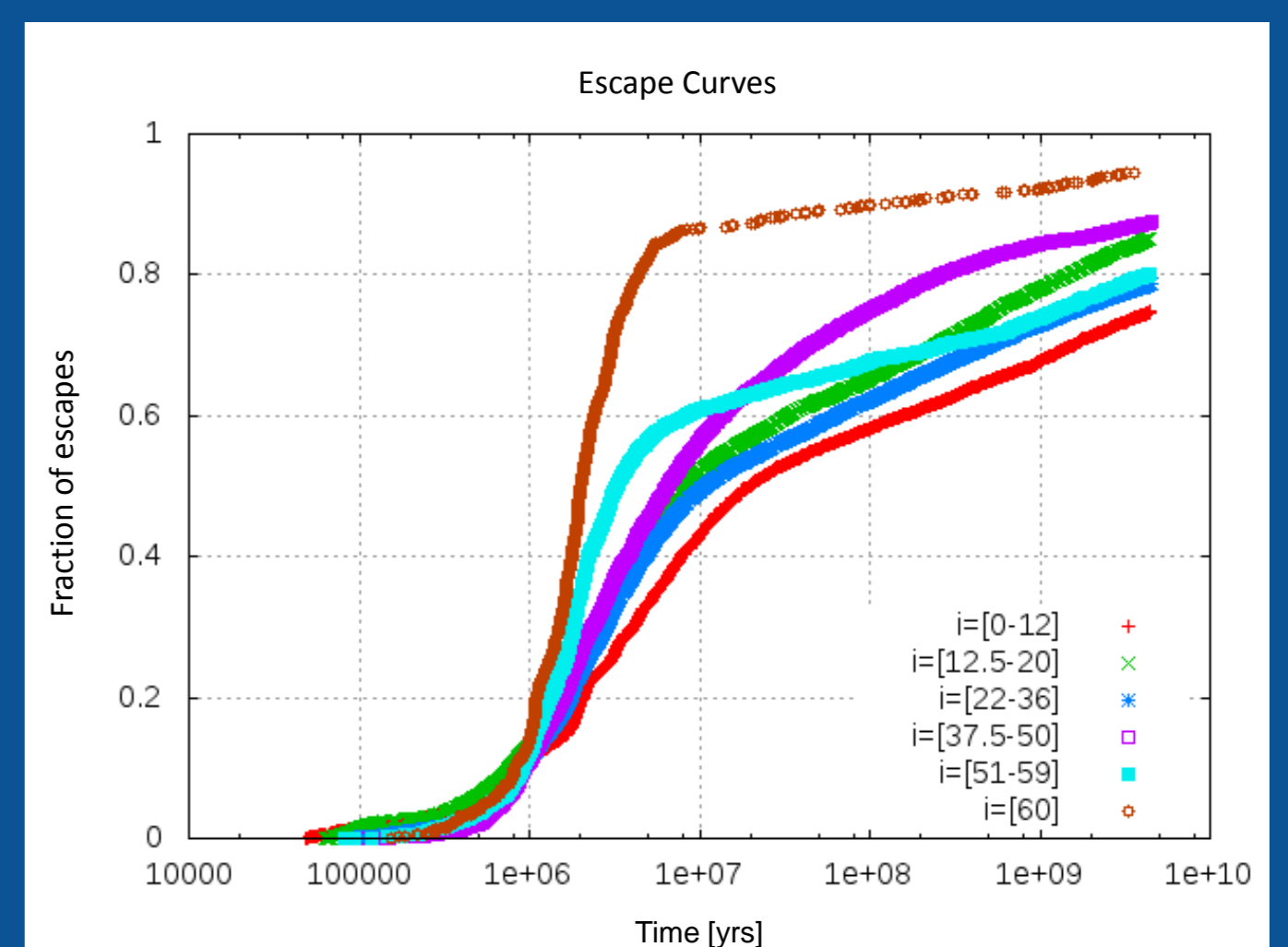
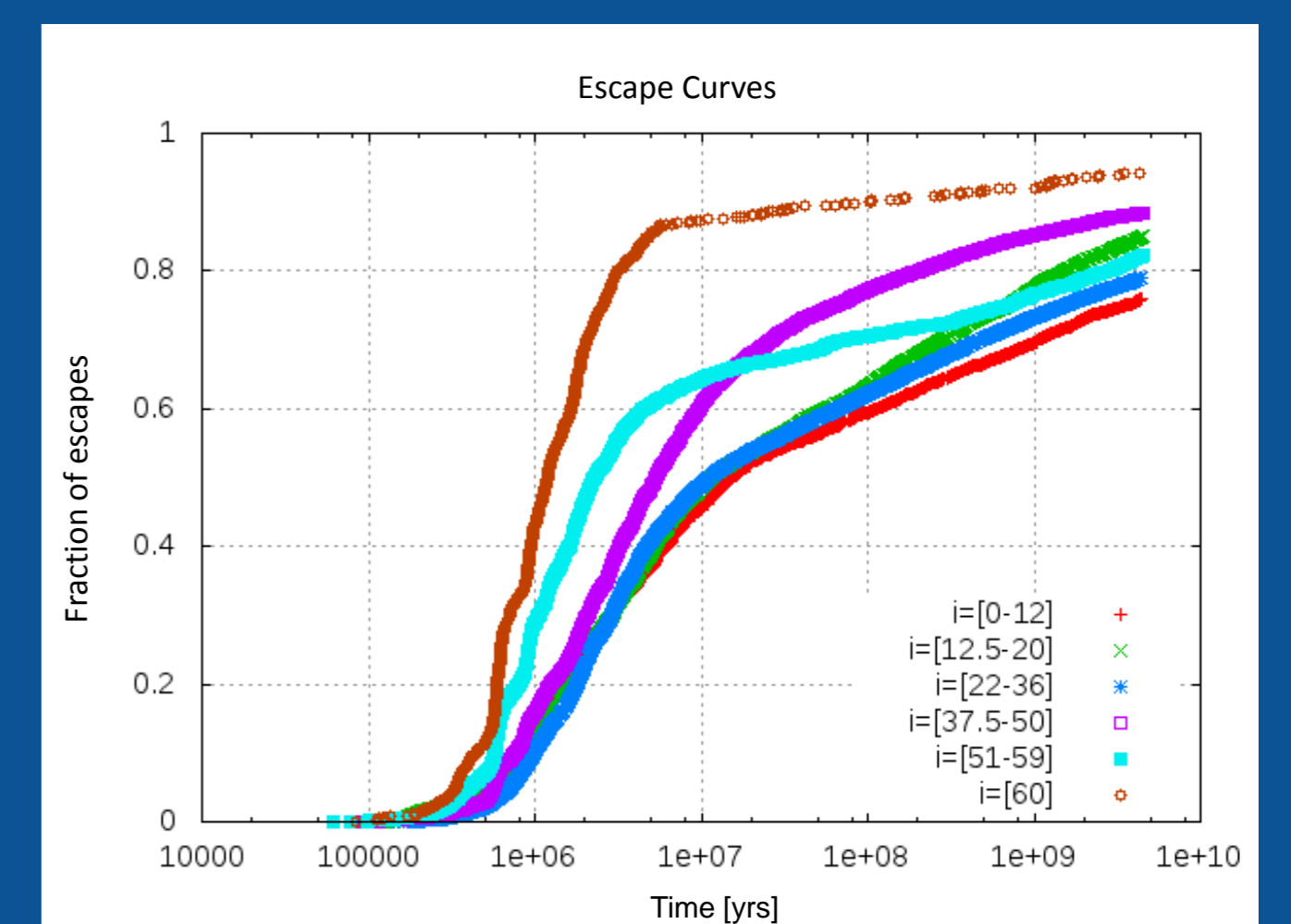


Figure 3: Top: Fraction of particles that escape according to stability zones around the Lagrangian point L<sub>4</sub>. Bottom: Fraction of particles that escape according to stability zones around the Lagrangian point L<sub>5</sub>.

From the output files of our simulation, we also perform stability maps, that are shown in Figure 4 and Figure 5 respectively. These maps show the normalized time fraction spent by the particles in our simulation. The color code is indicative of the portion of time or permanence time spent in each zone (blue for most visited regions, red for least visited). Note in particular the different stability zones in inclination defined by Zhou et al. (2009). It is also shown the six Trojans observed in L<sub>4</sub> (UP10, TO74, QR322, TN53, RJ103, VL305) and the three Trojans observed in L<sub>5</sub> (KV18, LC18, HM102) (see the orbital parameters in Table 1).

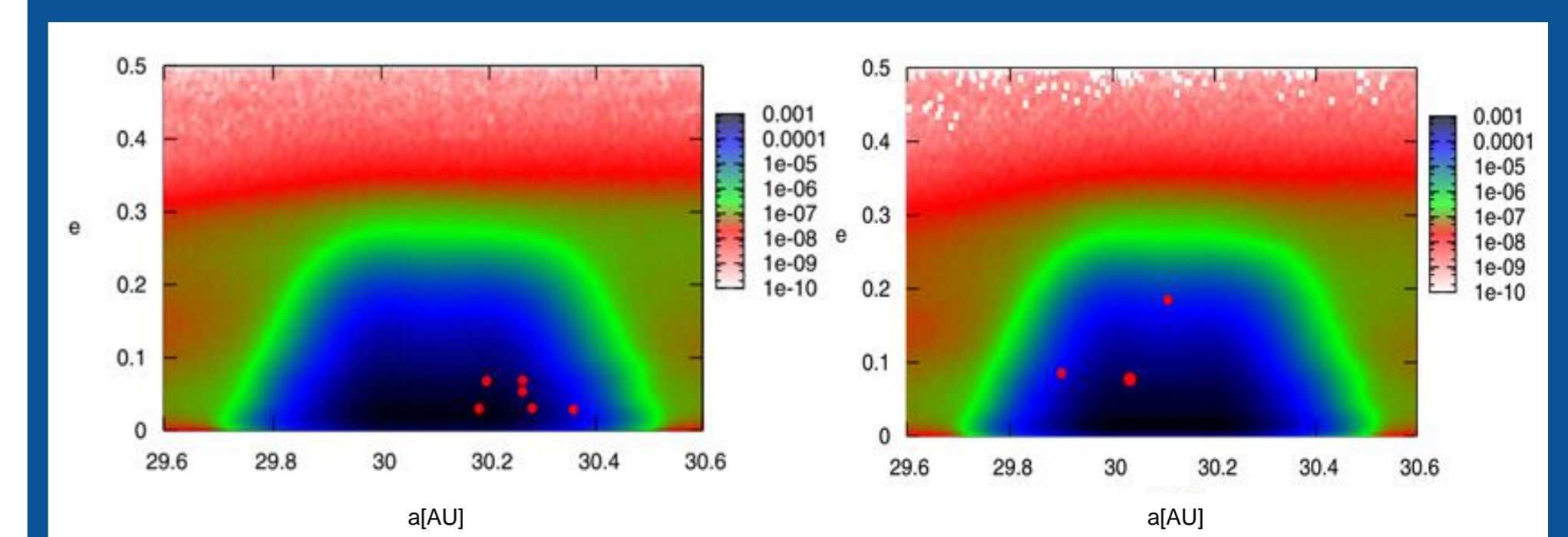


Figure 4: Left: Map of stability ( $a$  vs  $e$ ) around the Lagrangian point L<sub>4</sub>. Right: Map of stability ( $a$  vs  $e$ ) around the Lagrangian point L<sub>5</sub>. The color palette represent zones of different stability, being the blue color representative of the most stable regions.

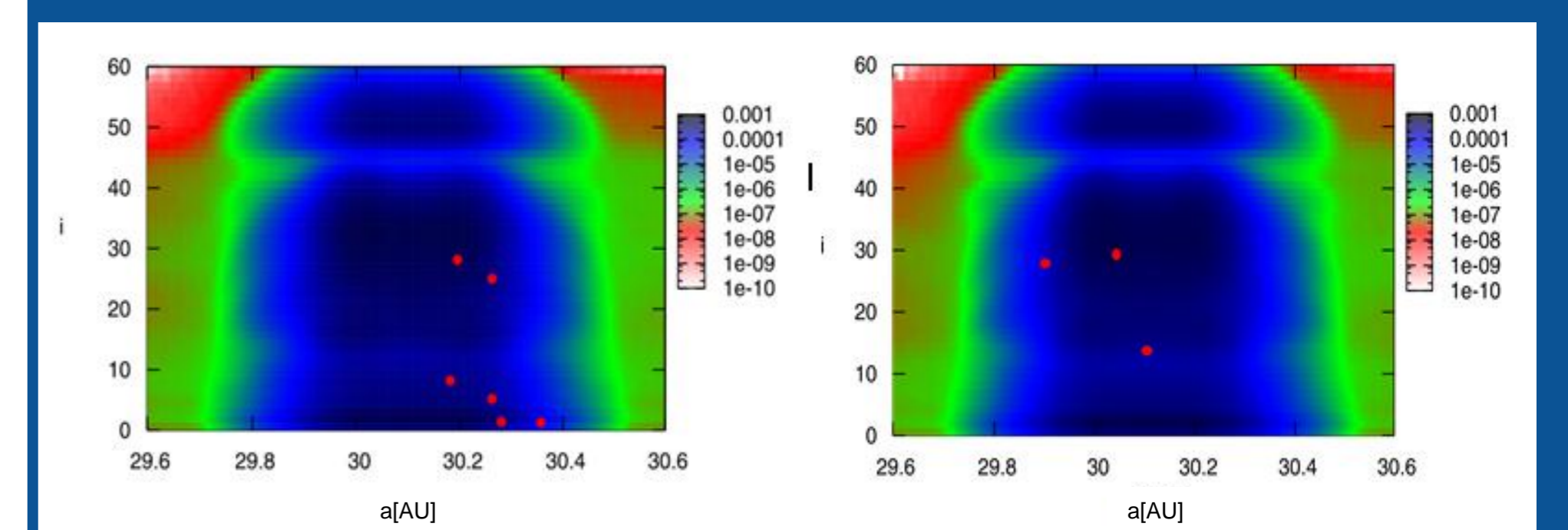


Figure 5: Left: Stability maps ( $a$  vs  $i$ ) around the Lagrangian point L<sub>4</sub>. Right: Stability maps ( $a$  vs  $i$ ) around the Lagrangian point L<sub>5</sub>. The color palette represents zones of different stability, being the blue one representative of the most stable regions.

## REFERENCES

- Sheppard, S., & Trujillo, C. 2010, ApJL,723,L233
- Zhou, L., Dvorak, R., & Sun, Y. 2009, MNRAS, 398,1217
- Zhou, L., Dvorak, R., & Sun, Y. 2011, MNRAS, 410,1849
- Fernandez J.A., Gallardo T., & Brunini A., 2002, Icarus,159, 358.

Contact:

Eduardo Tello Huanca, [elth@fcaglp.unlp.edu.ar](mailto:elth@fcaglp.unlp.edu.ar)